

Field and temperature dependence of remanent magnetization in a single crystal of $\text{Bi}_2\text{Sr}_2\text{CaCu}_2\text{O}_y$

Ming Xu

*Ames Laboratory and Iowa State University, Ames, Iowa 50011
and Materials Science Division, Argonne National Laboratory, Argonne, Illinois 60439*

A. Umezawa and G. W. Crabtree

Materials Science Division, Argonne National Laboratory, Argonne, Illinois 60439

(Received 4 May 1992)

We report the studies of the virgin and remanent magnetization in a single crystal of $\text{Bi}_2\text{Sr}_2\text{CaCu}_2\text{O}_y$ over a wide range of fields and temperatures. Based on the critical-state model, the field and temperature-dependence of the magnetization can be well understood. The first and second penetration fields have been estimated, based upon the measurements of the magnetization in a single crystal of $\text{Bi}_2\text{Sr}_2\text{CaCu}_2\text{O}_y$. Also discussed are flux pinning, applications of the critical-state model, and related issues in this material.

I. INTRODUCTION

Many irreversible magnetic properties have been observed in hard superconductors including both conventional and high- T_c superconductors. These irreversible magnetic phenomena depend upon the impurity phases, precipitates, and inhomogeneities present in materials. In the mixed state, an interaction exists between flux lines and defects. The free energy will be lower if the flux lines are trapped by the defects. Thus the magnetic behavior for hard superconductors exhibits a strong history dependence. Based on the framework of the critical-state model,¹⁻¹³ irreversible magnetization can be understood in terms of flux-pinning effects.

One manifestation of the irreversible magnetic properties in hard superconductors is remanent magnetization, namely, the residual magnetization after the applied field has been turned off. Since remanent magnetization is a measurement of the effective flux-pinning strength present in superconductors, it should depend upon both the temperature and applied field, as well as on the history of processing. Remanent magnetization as a function of temperature and field is very complicated usually, because the pinning situations of individual system vary differently. However, at least we can qualitatively understand the behavior of remanent magnetization based on critical-state models. For example, calculations of the remanent magnetization in various critical-state models were carried out,¹⁴ which show a different behavior of the remanent magnetization in various regions of the applied field. Therefore the measurement of remanent magnetization should be powerful technique to investigate the irreversible properties of hard superconductors.

In recent studies of high- T_c superconductors, many magnetic properties have been extensively investigated. High- T_c superconductors basically have layered crystal-line structures where the CuO_2 layers are recognized as

primarily responsible for electron conduction. These anisotropic structures have led to many unusual physical behaviors in these high- T_c superconductors, such as the existence of an irreversibility line, which separates two regions in the field-temperature phase diagram.^{15,16} Using magnetically reversible properties, some physical parameters can be estimated such as the critical fields, coherence length, free energy, and specific-heat jump.¹⁷⁻²¹ In the irreversible region, most efforts have included studies of the magnetic hysteresis, critical-current density, and flux creep or magnetic relaxation.^{15,16,22-30}

Regarding remanent magnetization studies in high- T_c superconductors, Yeshurun *et al.* measured the remanent magnetization and studied its dependence on the lateral geometrical length scale for grid patterning thin high- T_c crystals.³¹ McElfresh *et al.* discussed remanent magnetization, lower critical field, and surface barriers in an $\text{YBa}_2\text{Cu}_3\text{O}_x$ crystal.³² Felner *et al.* studied the angular dependence of the remanent magnetization in $\text{Bi}_2\text{Sr}_2\text{CaCu}_2\text{O}_y$ and $\text{YBa}_2\text{Cu}_3\text{O}_x$ single crystals.³³ Kolesnik, Skoskiewicz, and Igalson argued that the geometry of the sample may play an important role in the anisotropic properties.³⁴ The temperature dependence of the remanent magnetization in ceramic (Bi,Pb) 2:2:2:3 was studied by Job and Rosenberg.³⁵ All of these studies attempted to analyze the anisotropic behaviors^{33,34} or estimate the lower critical field H_{c1} (Refs. 32 and 35) in each specific system. However, a complete study of the relationship of remanent magnetization to field and temperature has not been reported yet.

The purpose of this work is to study systematically the field and temperature dependence of remanent and virgin magnetization in a single crystal of $\text{Bi}_2\text{Sr}_2\text{CaCu}_2\text{O}_y$. The magnetization is measured over a broad region of field and temperature. We discuss the flux-penetration fields and flux pinning, based on the measurement of remanent magnetization in the context of the critical-state model.

II. EXPERIMENTAL DETAILS

The crystal used in this study was grown by a self-flux method. The crystal, mass = 1.5 mg and $T_c = 87$ K, was selected for the magnetization measurements. The crystal is the shape of a flat plate with dimensions of 1.5 mm \times 1.6 mm \times 0.1 mm. The qualities of the sample were examined by x-ray diffraction, scanning electron microscopy, and superconducting transition measurements. Details of the sample preparation and characterization are described in Refs. 29 and 36.

Magnetization data were taken with a commercial superconducting quantum interference device (SQUID) magnetometer over a range of temperatures (5–80 K) and applied fields (0.1–50 kOe). Since we are interested in flux-pinning effects, we focus mainly on the temperature and field range below the irreversibility line. The magnetic measurement procedure is as follows. The samples were first warmed to above 130 K, to move any possible trapped flux lines away from the samples. The samples were then cooled in a zero magnetic field to a desired temperature T below the transition temperature T_c . The magnetic field was applied, and the virgin magnetization was measured in this field. The applied field then was turned off, and the remanent magnetization was measured. The same steps were repeated to measure the next data of the magnetization and remanent magnetization as a function of the applied field. The direction of the fields was chosen parallel to the c axis of the samples. A demagnetization factor of the sample was found to be about 0.9 for this orientation, which can cause a large change in the magnetization ($4\pi M$). The data shown below have not been corrected by the demagnetization factor.

During measurement, the scan length and field inhomogeneity of the magnetometer are important for an accurate value of the magnetic moment. The field strength changes slightly along the travel length of the sample. For reversible-magnetization measurements, the error is proportional to the field change, and so the effect is small. But the field gradient can read to erroneous results of the measurements if hysteresis effects are present.^{37–39} A sample can undergo minor hysteresis loops as the sample travels through the SQUID coils because of the inhomogeneous field.^{38,39} Even small inhomogeneities of the field can lead to a significant error and cause the M -vs- H curve to decrease, because the value of the field is much larger than the magnetization.^{38,39} Therefore we choose a scan length of 3 cm throughout our measurements, in which the field variation along the scan length remains less than 0.05%.^{38,40}

III. RESULTS AND DISCUSSION

A. Virgin magnetization and first penetration field H_1^*

Figure 1 shows the virgin-magnetization curve of a single crystal of $\text{Bi}_2\text{Sr}_2\text{CaCu}_2\text{O}_y$ at the various temperatures indicated up to a magnetic field of 10 kOe. As can be seen, the virgin magnetization exhibits a peak at all temperatures. As the temperature increases, the peak position shifts to a low-field region, indicating that the flux is

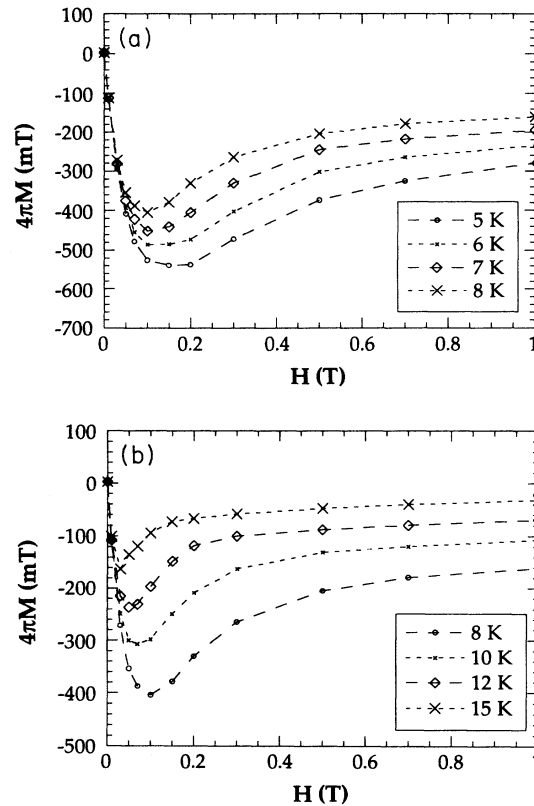


FIG. 1. Virgin magnetization vs applied field for a single crystal of $\text{Bi}_2\text{Sr}_2\text{CaCu}_2\text{O}_y$ at various temperatures (T): (a) $T = 5, 6, 7,$ and 8 K; (b) $T = 8, 10, 12,$ and 15 K. To show clearly the peak position, only the data are presented for a field region up to 10 kOe/1 T. The field is applied parallel to the c axis.

easier to move in the sample at higher temperatures. The penetration field (H_1^*), where the sample is first fully penetrated by the external field, can be estimated from the peak position for each temperature in terms of the critical-state model.

In the critical-state model, if J_c is assumed independent of the field, the magnetization is constant with an increasing field after the first penetration field.¹ In the field-dependent J_c relations, however, there is a peak position in the calculated virgin-magnetization curve.^{3–13} But detailed calculations⁴¹ show that the peak position is not the first penetration field, according to the field-dependent J_c relations. Both calculations and experiments indicate that the full penetration field is always higher than estimated from the peak of magnetization.⁴¹ One reason for this difference is that the boundary conditions, including the lower critical field, surface barrier, and equilibrium magnetization, have been ignored to simplify mathematics during most critical-state calculations.^{42–44} These boundary conditions will shift the full penetration field to a lower value closer to the peak position in the magnetization. However, experimentally one can qualitatively approximate the peak position as the value of the first penetration field for a system with lower values of H_{c1} and surface barrier. We show below that the corrections to these factors in $\text{Bi}_2\text{Sr}_2\text{CaCu}_2\text{O}_y$ may be

less important than in $\text{YBa}_2\text{Cu}_3\text{O}_x$. This treatment gives a correct physical picture and is reasonable, at least in qualitative discussions. Thus we can choose the first penetration field H_1^* as a peak position on the plot of virgin magnetization versus field.

It should be noted that the penetration field depends upon both the temperature and sample size.¹⁴ Actually, regardless of the quantitative relation of $H_1^*(T)$ to temperature, $H_1^*(T)$ is always a decreasing function of temperature. In other words, the sample in a constant field is more easily penetrated at higher temperatures. The reason is flux-pinning effects become weaker at higher temperature and then the flux is easier to move in the sample. In addition, a small sample would be easier for the magnetic field to fully penetrate at the same magnitude of the external magnetic field.

According to the virgin-magnetization measurement in the present single crystal of $\text{Bi}_2\text{Sr}_2\text{CaCu}_2\text{O}_y$, we estimate the penetration field H_1^* . The values of H_1^* vary from 0.17 T at 5 K to 0.03 T at 15 K for this sample.

B. Field dependence of remanent magnetization and second penetration field H_2^*

We show remanent magnetization versus the applied field at a given temperature for a single crystal of $\text{Bi}_2\text{Sr}_2\text{CaCu}_2\text{O}_y$ in Fig. 2. As can be seen from the figure, the remanent magnetization increases with the maximum applied field and then crosses over to a saturation value at higher fields. Saturation values of the fields depend upon temperature. Although our data were measured over the entire region of 5 T, here we only present data up to 1 T because there is no change in the remanent magnetization at the higher-field regions between 1 and 5 T.

As mentioned above, remanent magnetization is a measurement of flux-pinning effects in superconductors. Since the critical-state model quantitatively describes the irreversible magnetization,¹⁻⁹ both field and temperature dependence of remanent magnetization can be predicted in this picture.¹⁴ But because of complicated pinning situations in real materials, different pinning mechanisms will create quite different irreversible-magnetic properties. For example, there exist several versions of the critical-state relations to describe quantitatively individual systems.¹⁻⁹ Based on these critical-state models, remanent magnetization can be calculated and predicted in terms of several structurally related parameters involved in critical-state models.^{11,14,31,32} Reference 14 shows that remanent magnetization has three different stages, distinguished by two characteristic penetration fields. In the first stage, the remanent magnetization has a relatively small value, as a result of partial penetration, while the maximum field (H_m) is smaller than the first penetration field (H_1^*), as shown in Fig. 3(a).

Besides the first penetration field (H_1^*), the second penetration field (H_2^*) is another important characteristic field. This field is defined as the external field, while there is no contribution from the increasing branch of the local field to the remanent magnetization.¹⁴ In the second stage ($H_1^* < H_m < H_2^*$), the remanent magnetization is a

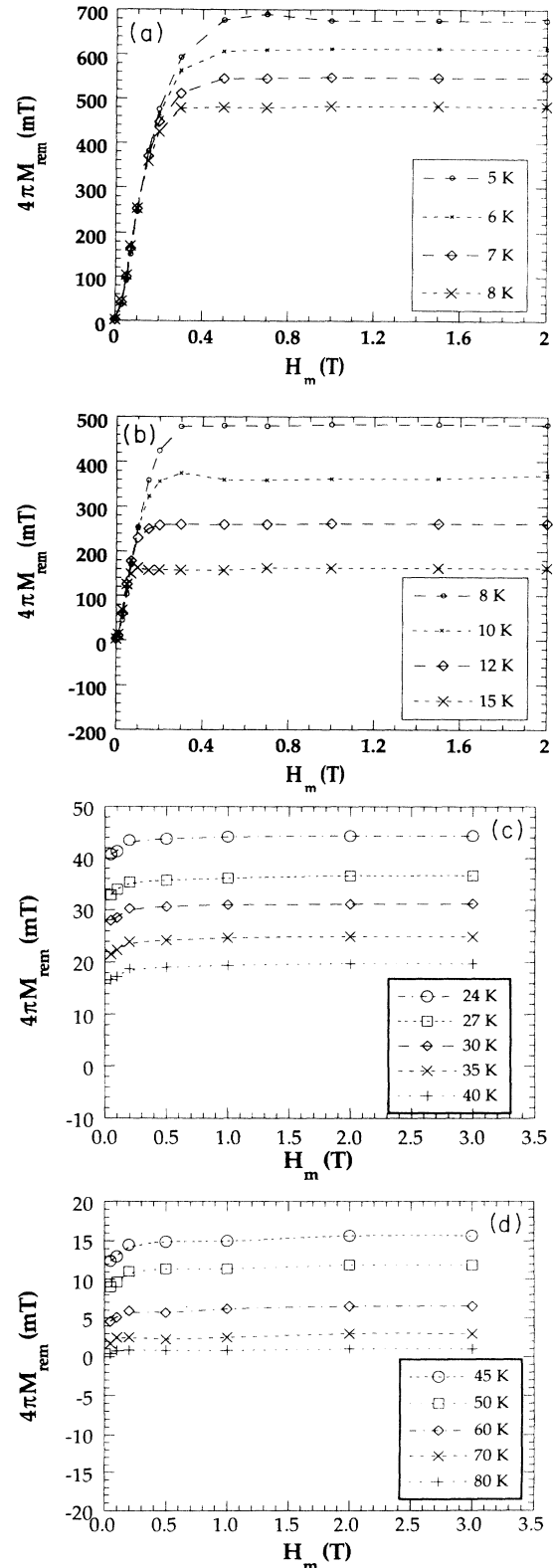


FIG. 2. Remanent magnetization (M_{rem}) vs maximum applied field (H_m) for a single crystal of $\text{Bi}_2\text{Sr}_2\text{CaCu}_2\text{O}_y$ at various temperatures (T): (a) $T=5, 6, 7,$ and 8 K; (b) $T=8, 10, 12,$ and 15 K; (c) $T=24, 27, 30, 35,$ and 40 K; (d) $T=45, 50, 60, 70,$ and 80 K. To show clearly the peak position, only data are presented for a field region up to 2 T/3.5 T. The field is applied parallel to the c axis.

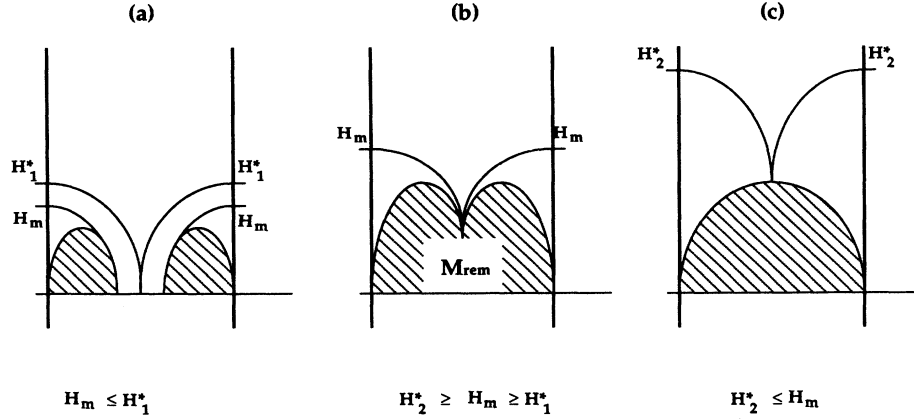


FIG. 3. Local field distribution for a slab in an applied field parallel to the surface of the slab in the critical-state model for the three stages: (a) $H_m < H_1^*$, (b) $H_1^* < H_m < H_2^*$, and (c) $H_m > H_2^*$. Solid curves represent the local field for the increasing branch after turning on a maximum applied field H_m . Shaded areas represent the remanent magnetization after turning off the applied field and show the total flux trapped in the material.

complicated function of the applied field. The expression of the remanent magnetization depends upon the version of the critical-state relation. As illustrated in Fig. 3(b), both increasing and decreasing local fields contribute to the remanent magnetization significantly during this stage.

Moreover, as the applied field is beyond the second penetration field ($H_m > H_2^*$), the remanent magnetization does not vary with the applied field and only depends upon sample size, geometry, and material parameters or temperature.¹⁴ Although each critical-state relation results in a different magnitude of the remanent magnetization, the field independence is a common property in this region. This saturation property of remanent magnetization can be understood from Fig. 3(c).

Thus we can summarize the above properties of remanent magnetization as follows:

$$\begin{aligned}
 & (d/x_0)f_1(H_m/H_0) \text{ for } H_m \leq H_1^* , \\
 & 4\pi M_{\text{rem}}/H_0 = f_2(d/x_0, H_m/H_0) \\
 & \quad \text{for } H_1^* \leq H_m \leq H_2^* , \quad (1) \\
 & f_3(d/x_0) \text{ for } H_m \geq H_2^* ,
 \end{aligned}$$

where the remanent magnetization is normalized by the parameter $H_0(T)$ involved in the critical-state relations, d is the half width of the superconducting slab with an external field parallel to the surface of the slab, x_0 is the reduced parameter with a dimension of the length, $x_0(T) = cH_0(T)/4\pi J_c(T)$, where $J_c(T)$ is the temperature-dependent critical-current density in the critical-state relations, and $f_i(x)$ is a function depending upon the critical-state relation and different field stages ($i = 1, 2, 3$).

In order to compare the theoretical curve of remanent magnetization with the experimental data, we plot remanent magnetization versus field in the normalized scale by H_0 for the two different temperatures, based on

the calculations of the linear critical-state relation. We have chosen $J_c(T) = 10^5$ A/cm², $d = 0.5$ mm, and $H_0 = 0.5$ T for low temperature and 1.0 T for high temperature, respectively, in Fig. 4(a). We have also plotted

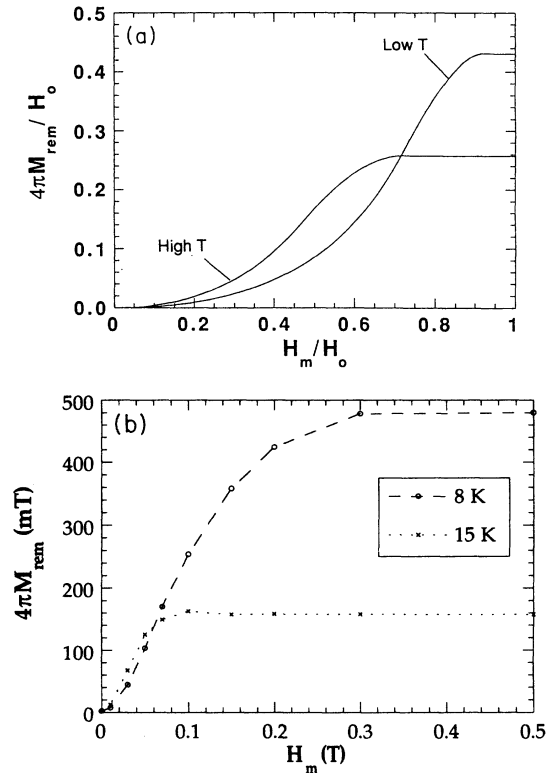


FIG. 4. Comparison of the curves of experimental and calculated remanent magnetization (M_{rem}) vs maximum applied field (H_m): (a) calculated results based on a field-dependent critical-state model as mentioned in the text; (b) observed data for temperatures of 8 and 12 K. Note that (1) a saturated M_{rem} after the second penetration field appears and (2) a crossover of M_{rem} for different temperatures happens in both curves. Also note that M_{rem} increases quite rapidly at low H_m for 8 and 12 K in the measured curve.

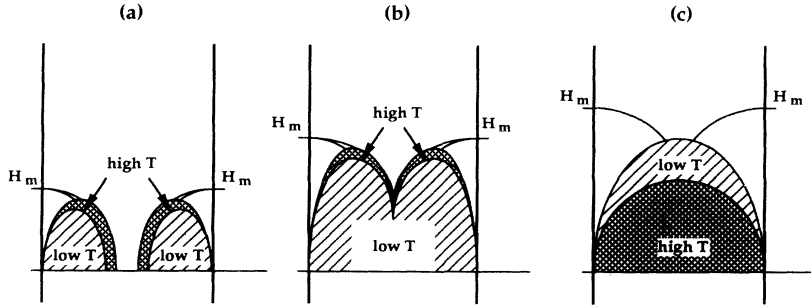


FIG. 5. Temperature effects on the local field distribution for a slab in an applied field parallel to the surface of the slab in the critical-state model for the three stages: (a) $H_m < H_1^*(T)$, (b) $H_1^*(T) < H_m < H_2^*(T)$, and (c) $H_m > H_2^*(T)$, in which the maximum applied field (H_m) is kept unchanged for zero-field-cooled processing. Shaded areas represent the remanent magnetization after turning off the applied field and show the total flux trapped in the material.

the experimental data of remanent magnetization in a single crystal of $\text{Bi}_2\text{Sr}_2\text{CaCu}_2\text{O}_y$ at 8 and 12 K within a smaller field scale in Fig. 4(b). As can be seen from these figures, good agreement between these curves has been reached, at least qualitatively.

As reported in Ref. 32, in the low-field limit, M_{rem} is virtually zero in a single crystal of $\text{YBa}_2\text{Cu}_3\text{O}_x$. The magnitude of $4\pi M_{\text{rem}}$ is about several gauss for $H_{\parallel c}$ up to 1 kOe of the applied field at 8 K in a single crystal of $\text{YBa}_2\text{Cu}_3\text{O}_x$. But as shown in Figs. 2 and 4(b) in a single crystal of $\text{Bi}_2\text{Sr}_2\text{CaCu}_2\text{O}_y$, this low-field-independent property disappears instead of a rapid enhancement of M_{rem} with an increasing H_m . We noticed that the sample dimensions of the $\text{YBa}_2\text{Cu}_3\text{O}_x$ of Ref. 32 were even smaller than those of our $\text{Bi}_2\text{Sr}_2\text{CaCu}_2\text{O}_y$. Thus this difference cannot come from dimension variation instead of the boundary conditions including H_{c1} , surface barrier, and equilibrium magnetization near the surface of the sample. It has been recognized that the low critical field is smaller in $\text{Bi}_2\text{Sr}_2\text{CaCu}_2\text{O}_y$ than in $\text{YBa}_2\text{Cu}_3\text{O}_x$ (Refs. 18 and 28) and the surface barrier is important in $\text{YBa}_2\text{Cu}_3\text{O}_x$ for flux pinning.⁴⁵ In addition, critical-state calculations show that a correction of the boundary conditions will shift the zero value of this low-field M_{rem} to a higher field. Therefore it may be a better approximation for $\text{Bi}_2\text{Sr}_2\text{CaCu}_2\text{O}_y$ to take the boundary condition excluding these corrections. This implies that the contribution to the remanent magnetization from the H_{c1} , surface barrier, and equilibrium magnetization could be very small and an estimation of H_{c1} from the M_{rem} measurement is very difficult in the $\text{Bi}_2\text{Sr}_2\text{CaCu}_2\text{O}_y$ system.

Experimentally, since there does not exist a clear boundary to distinguish the first and second stages characterized by H_1^* in the remanent magnetization data, it is not easy to determine the first penetration field in the remanent magnetization measurement [see Figs. 2 and 4(b), for example]. But it will be very apparent to estimate the second penetration field H_2^* from the measurement of remanent magnetization, from which we can find the second penetration field as a function of temperature. The values of H_2^* vary from 0.50 T at 5 K to 0.10 T at 15 K for the present single crystal of $\text{Bi}_2\text{Sr}_2\text{CaCu}_2\text{O}_y$. As mentioned above, both H_1^* and H_2^* depend upon the sample size. We do not attempt to make a further analysis on the penetration fields.

C. Temperature dependence of remanent magnetization

In Fig. 5 we exhibit remanent magnetization versus temperature data at several given fields (H_m) for a single crystal of $\text{Bi}_2\text{Sr}_2\text{CaCu}_2\text{O}_y$. At low H_m from 0.05 to 0.5 T in Fig. 5(a), the remanent magnetization slightly increases with an increasing temperature and then joins a universal curve, where the remanent magnetization becomes independent of the H_m . At high H_m above 0.5 T as shown in Fig. 5(b), however, the remanent magnetization ap-

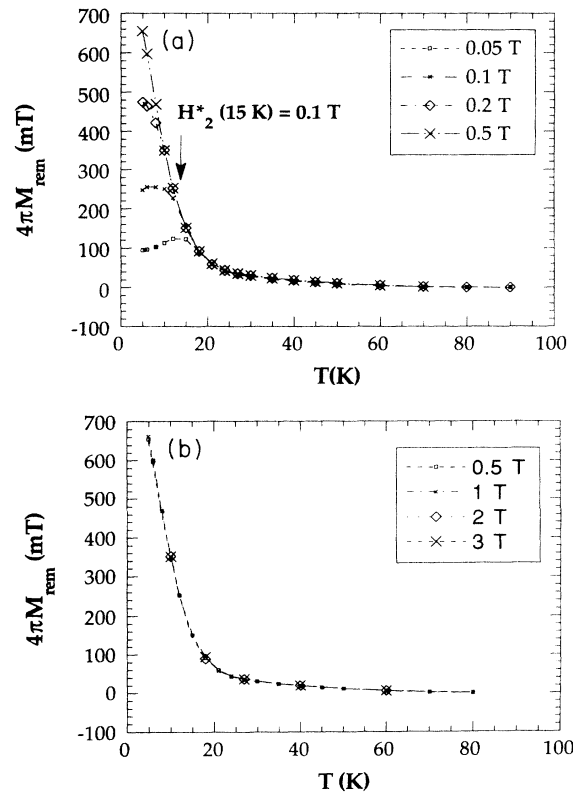


FIG. 6. Remanent magnetization (M_{rem}) vs temperature (T) for a single crystal of $\text{Bi}_2\text{Sr}_2\text{CaCu}_2\text{O}_y$ at a constant maximum applied field (H_m): (a) $H_m = 0.05, 0.1, 0.2,$ and 0.5 T; (b) $H_m = 0.5, 1, 2,$ and 3 T. The field is applied parallel to the c axis in zero-field-cooled processing.

pears to be independent of H_m .

According to the critical-state model, $H_2^*(T)$ is a decreasing function with increasing temperature, since the flux penetrates the sample more favorably at higher temperatures. Once H_m reaches H_2^* , the remanent magnetization will be saturated, from which we can understand the common part of M_{rem} versus temperature at a higher-temperature region. Before the second full penetration, the flux trapped by the defects in the sample will increase with increasing temperature, as illustrated in Figs. 6(a) and 6(b). But after reaching $H_2^*(T)$, the trapped flux will be rapidly excluded with an increasing temperature, as shown in Fig. 6(c), which implies a rapidly decreasing M_{rem} with increasing temperature. Therefore we can interpret why the remanent magnetization slightly increases and then joins the common part at the low- H_m region. In the high- H_m region (≥ 0.5 T), since the sample is closely penetrated by $H_2^*(T)$, the remanent magnetization remains saturated with varying temperatures. Therefore, in this part, M_{rem} does not depend upon H_m and rapidly decreases with a rising temperature.

IV. CONCLUSIONS

We have investigated virgin and remanent magnetization in irreversible regions for a single crystal of $\text{Bi}_2\text{Sr}_2\text{CaCu}_2\text{O}_y$. Based on the critical-state model, we can understand the temperature and field dependence of virgin and remanent magnetization. The first penetration field can be experimentally estimated from the peak posi-

tion in the virgin-magnetization curve. In the field dependence of the remanent magnetization, the second penetration field can be chosen where the remanent magnetization first reaches saturation. From an experimental point of view, we can distinguish the first penetration field in the virgin-magnetization data and the second penetration field in the remanent magnetization. The experimental observation of the field dependence of remanent magnetization can be predicted by critical-state calculations. The data show that the boundary conditions during critical-state calculations are important, but these conditions can be ignored in a single crystal of $\text{Bi}_2\text{Sr}_2\text{CaCu}_2\text{O}_y$, indicating the small values of H_{c1} , weak surface barrier, and possible low equilibrium magnetization in this system. The temperature dependence of remanent magnetization can also be qualitatively understood in terms of temperature effects on the critical-state model.

ACKNOWLEDGMENTS

The authors are grateful to D. K. Finnemore and H. W. Weber for stimulating discussions during this work. Ames Laboratory is operated for the U.S. Department of Energy by Iowa State University under Contract No. W-7405-ENG-82. This work was supported by the Department of Energy under Grant No. DE-FG02-90ER45427 through the Midwest Superconductivity Consortium and the Office of Basic Energy Sciences. The work at Argonne was supported by the U.S. Department of Energy, Basic Energy Sciences-Materials Sciences, under Contract No. W-31-109-ENG-38.

-
- ¹C. P. Bean, Phys. Rev. Lett. **8**, 250 (1962); Rev. Mod. Phys. **36**, 31 (1964).
²H. London, Phys. Lett. **6**, 162 (1963).
³Y. B. Kim, C. F. Hempstead, and A. R. Strnad, Phys. Rev. Lett. **9**, 306 (1962); Phys. Rev. **129**, 528 (1963).
⁴H. A. Ullmaier and R. H. Kernohan, Phys. Status Solidi **17**, K223 (1966).
⁵F. Irie and K. Yamafuji, J. Phys. Soc. Jpn. **23**, 255 (1967).
⁶W. A. Fietz, M. R. Beasley, J. Sicox, and W. W. Webb, Phys. Rev. **136**, A335 (1964).
⁷V. R. Karasik, N. G. Vasil'ev, and V. G. Ershov, Zh. Eksp. Teor. Fiz. **59**, 790 (1970) [Sov. Phys. JETP **32**, 433 (1970)].
⁸J. H. P. Watson, J. Appl. Phys. **39**, 3406 (1968).
⁹A. M. Campbell and J. E. Evetts, Adv. Phys. **21**, 199 (1972).
¹⁰W. E. Timms, Phys. Lett. **40A**, 427 (1972); J. R. Cave, J. E. Evetts, and A. M. Compell, J. Phys. (Paris) Colloq. **29**, C6-614 (1978).
¹¹P. Chaddah and G. Ravi Kumar, Phase Transit. **19**, 37 (1989); G. Ravi Kumar and P. Chaddah, Phys. Rev. B **39**, 4704 (1989).
¹²D.-X. Chen and R. B. Goldfarb, J. Appl. Phys. **66**, 2489 (1989); D.-X. Chen, A. Sanchez, and J. S. Munoz, *ibid.* **67**, 3430 (1990); D.-X. Chen, A. Sanchez, J. Nogues, and J. S. Munoz, Phys. Rev. B **41**, 9510 (1990).
¹³M. Xu, D. Shi, and R. F. Fox, Phys. Rev. B **42**, 10 773 (1990).
¹⁴M. Xu, Phys. Rev. B **44**, 2713 (1991).
¹⁵K. A. Muller, M. Takashige, and J. G. Bednorz, Phys. Rev. Lett. **58**, 1143 (1987).
¹⁶Y. Yeshurun and A. P. Malozemoff, Phys. Rev. Lett. **60**, 2202 (1988); Y. Yeshurun, A. P. Malozemoff, F. H. Holtzberg, and T. R. Dinger, Phys. Rev. B **38**, 11 828 (1988).
¹⁷L. Krusin-Elbaum, A. P. Malozemoff, Y. Yeshurun, D. C. Cronmeyer, and F. H. Holtzberg, Phys. Rev. B **39**, 2936 (1989); L. Krusin-Elbaum, R. L. Greene, F. H. Holtzberg, A. P. Malozemoff, and Y. Yeshurun, Phys. Rev. Lett. **62**, 217 (1989).
¹⁸A. Umezawa, G. W. Crabtree, J. Z. Liu, T. J. Moran, S. K. Malik, L. H. Nunez, W. L. Kwok, and C. H. Sowers, Phys. Rev. B **38**, 2843 (1988); A. Umezawa, G. W. Crabtree, U. Welp, W. L. Kwok, K. G. Vandervoort, and J. Z. Liu, *ibid.* **42**, 8744 (1990).
¹⁹U. Welp, W. L. Kwok, G. W. Crabtree, K. G. Vandervoort, and J. Z. Liu, Phys. Rev. Lett. **62**, 1908 (1989); J. Gohng and D. K. Finnemore, Phys. Rev. B **46**, 398 (1992).
²⁰P. H. Kes, C. J. van der Beek, M. P. Maley, M. E. McHenry, D. A. Huse, M. J. V. Menken, and A. A. Menovsky, Phys. Rev. Lett. **67**, 2383 (1991); W. Kraitschka, F. M. Sauerzopf, and H. W. Weber, Physica C **179**, 59 (1991); Q. Li, M. Suenaga, J. Gohng, D. K. Finnemore, T. Hikata, and K. Sato (unpublished).

- ²¹J. Gohng and D. K. Finnemore, Phys. Rev. B **42**, 7946 (1990); S. C. Sanders, O. B. Hyun, and D. K. Finnemore, *ibid.* **42**, 8035 (1990).
- ²²A. Umezawa, G. W. Crabtree, J. Z. Liu, H. W. Weber, W. K. Kwok, L. H. Nunez, T. J. Moran, and C. H. Sowers, Phys. Rev. B **36**, 715 (1988).
- ²³A. P. Malozemoff, in *Physical Properties of High Temperature Superconductors I*, edited D. M. Ginsberg (World Scientific, Singapore, 1989).
- ²⁴H. W. Weber, in *Studies of High Temperature Superconductors*, edited by A. V. Narlikar (Nova Scientific, New York, 1989), Vol. 3.
- ²⁵H. W. Weber and G. W. Crabtree, in *Studies of High Temperature Superconductors*, edited by A. V. Narlikar (Nova Scientific, New York, 1991), Vol. 9.
- ²⁶P. Chaddah, Pramana J. Phys. **36**, 353 (1991).
- ²⁷Y. Yeshurun, A. P. Malozemoff, T. K. Worthington, R. M. Yandroski, L. Krusin-Elbaum, F. H. Holtzberg, T. R. Dinger, and G. V. Chandrashekar, Cryogenics **29**, 258 (1989).
- ²⁸T. T. M. Palstra, B. Batlogg, L. F. Schneemeyer, and J. V. Waszczak, Phys. Rev. Lett. **61**, 1662 (1988); T. T. M. Palstra, B. Batlogg, R. B. van Dover, L. F. Schneemeyer, and J. V. Waszczak, Appl. Phys. Lett. **54**, 763 (1989); Phys. Rev. B **41**, 6621 (1990).
- ²⁹M. Xu and D. Shi, Physica C **168**, 303 (1990); D. Shi, M. Xu, A. Umezawa, and R. F. Fox, Phys. Rev. B **42**, 2062 (1990); M. Xu, D. Shi, A. Umezawa, K. G. Vandervoort, and G. W. Crabtree, *ibid.* **43**, 13 049 (1991).
- ³⁰J. P. Rice, D. M. Ginsberg, M. W. Rabin, K. G. Vandervoort, G. W. Crabtree, and H. Claus, Phys. Rev. B **41**, 6532 (1990); V. V. Moshchalkov, A. A. Gippius, A. A. Zhukov, H. H. Nyan, V. I. Voronkova, and V. K. Yanovskii, Physica C **165**, 62 (1990).
- ³¹Y. Yeshurun, M. W. McElfresh, A. P. Malozemoff, J. Hagerhorst-Trehwella, J. Mannhart, F. Holtzberg, and G. V. Chandrashekar, Phys. Rev. B **42**, 6322 (1990).
- ³²M. W. McElfresh, Y. Yeshurun, A. P. Malozemoff, and F. Holtzberg, Physica A **168**, 308 (1990).
- ³³I. Felner, U. Yaron, Y. Yeshurun, G. V. Chandrashekar, and F. Holtzberg, Phys. Rev. B **40**, 5239 (1989); I. Felner, U. Yaron, and Y. Yeshurun, *ibid.* **43**, 13 681 (1991).
- ³⁴S. Kolesnik, T. Skoskiewicz, and J. Igalson, Phys. Rev. B **43**, 13 679 (1991).
- ³⁵Ch. J. Liu, R. Buder, C. Escribe-Filippini, J. Marcus, P. L. Reydet, B. S. Mathis, and C. Schlenker, Physica C **162-164**, 1609 (1989); V. V. Moshchalkov, O. V. Petrenko, A. A. Zhukov, A. A. Gippius, V. I. Voronova, V. S. Belov, and V. A. Rybachuk, *ibid.* **162-164**, 1611 (1989); R. Job and M. Rosenberg, *ibid.* **172**, 391 (1991).
- ³⁶J. Z. Liu, G. W. Crabtree, L. E. Rehn, Urs Geiser, D. A. Young, W. K. Kwok, P. M. Baldo, J. M. Williams, and D. J. Lam, Phys. Lett. A **127**, 444 (1988); D. Shi, M. Tang, Y. C. Chang, P. Z. Jiang, K. Vandevoot, B. Malecki, and D. J. Lam, Appl. Phys. Lett. **54**, 2358 (1989).
- ³⁷Y. Xu, M. Suenaga, A. R. Moodenbaugh, and D. O. Welch, Phys. Rev. B **40**, 10 882 (1989); K. S. Lichtenberger, Ph.D. thesis, Iowa State University, 1991.
- ³⁸G. M. Stollman, B. Dam, J. H. P. M. Emmen, and Pankert, Physica C **161**, 444 (1989).
- ³⁹K. Togano, H. Kumakura, J. Kase, Q. Li, J. E. Osterson, and D. K. Finnemore, J. Appl. Phys. **70**, 6966 (1991).
- ⁴⁰See, for example, Quantum Design MPMS SQUID manual.
- ⁴¹M. Xu (unpublished); H. Wiesinger and H. W. Weber (unpublished).
- ⁴²J. R. Clem, J. Appl. Phys. **50**, 3518 (1979).
- ⁴³L. Krusin-Elbaum, A. P. Malozemoff, D. C. Cronmeyer, F. Holtzberg, J. R. Clem, and Z. Hao, J. Appl. Phys. **67**, 4670 (1990).
- ⁴⁴J. R. Cave, Supercond. Sci. Technol. **5**, S399 (1992).
- ⁴⁵M. Konczykowski, L. Burlachkov, Y. Yeshurun, and F. Holtzberg, Phys. Rev. B **43**, 13707 (1991); L. Burlachkov, M. Konczykowski, Y. Yeshurun, and F. Holtzberg (unpublished).